

Kinetics for Hydrocracking Based on Structural Classes: Model Development and Application

G. G. Martens and G. B. Marin

Laboratorium voor Petrochemische Techniek, Universiteit Gent, B-9000 Gent, Belgium

A kinetic model for hydrocracking of an industrial feedstock, fully incorporating the carbenium ion chemistry, was developed. Individual hydrocarbons in the reaction network were relumped into 8 lumps per carbon number: n-alkane, mono-, di- and tri-branched alkanes, mono-, di-, tri- and tetraring cycloalkanes. The rate coefficient of a reaction in the relumped network resulted from the product of the rate coefficients of the elementary reaction steps with lumping coefficients. The former were obtained from regressions on gas-phase hydrocracking data of model components. Lumping coefficients were calculated based on the assignment of all (cyclo)alkanes and the corresponding carbenium ions to structural classes comprising species with identical thermodynamic properties. The simulation of an industrial reactor with vacuum gas-oil feed revealed the relative unimportance of transfer limitations for hydrocracking of saturated hydrocarbons and the model's ability to detail the influence of process conditions on the product composition.

Introduction

The kinetic models most widely used in the design and control of hydroprocessing (Stangeland and Kitrell, 1972; Quader et al., 1970), catalytic cracking (Jacob et al., 1976; Weekman and Nace, 1970) or catalytic reforming (Marin and Froment, 1990) often consider only a limited number of so-called lumps representing the refinery's major product fractions and containing a whole spectrum of hydrocarbons. The success of these models lies in their ease of application and incorporation into a reactor model, considering the limited number of reactions and corresponding rate parameters involved. The price to be paid for this simplicity is often a dependency of the rate parameters on the feedstock composition requiring a time-consuming adjusting of their values for each new feedstock. Moreover, few or no details are known concerning the detailed molecular composition determining the quality of the products obtained. A step towards the recognition of the chemical and physical diversity of the numerous hydrocarbons in a typical feedstock is the use of continuous lumping models (Cicarelli et al., 1992; Krambeck, 1994; Laxminarasimhan et al., 1996) describing the physical properties and reaction rates as a continuous function of a measurable variable such as boiling point or molecular weight.

Although exhibiting better predictive capabilities with respect to product yield and quality rather than discrete lumping models, they still lack the incorporation of the underlying reaction chemistry. Quann and Jaffe (1992, 1996) introduced fundamental reaction chemistry into a lumped model by considering each hydrocarbon as an assembly of a limited number of structural building units. Hydrocarbons comprising the same structural features are assumed to have the same physical properties, as well as identical chemical reaction behavior allowing them to be collected in the same lump. Respecting the fundamental chemistry, a limited number of reaction rules are introduced for each group of structurally related components. A similar strategy is used by Liguras and Allen (1989a,b) who consider each hydrocarbon as a collection of distinct carbon centers whereby the reaction behavior of the individual components is derived from the reaction behavior of its carbon centers. Each lump is hereby represented by what they call pseudo components, and the rates of the various reactions between the pseudo components are calculated from group contributions for the different carbon centers considered, for which values are obtained from experimental data on pure components.

The only models reported in literature who consider in full detail the underlying chemistry for the individual hydrocar-

Correspondence concerning this article should be addressed to G. B. Marin.

bon species are the fundamental kinetic models. Klein and coworkers developed kinetic models for pyrolysis of alkanes and cycloalkanes (Broadbeldt et al., 1994) and catalytic cracking (Watson et al., 1996, 1997a,b) starting from a reaction network of elementary reaction steps generated by implementation of the known chemistry rules into a computer algorithm. The numerous kinetic parameters associated with the reaction steps were reduced to a manageable set using linear free energy relations which relate the rate coefficient of each step to a so-called reactivity index the value of which is obtained from quantumchemical calculations.

The model discussed in this article is based on an approach originally developed for thermal cracking (Clymans and Froment 1984; Hillewaert et al., 1988) and further modified to be applied to reactions catalyzed by solid acids (Baltanas et al., 1989). Generation of the reaction network occurs using a computer algorithm in which each species is represented by a boolean relationship matrix. The kinetic rate coefficient of each elementary step is expressed as a multiple of single event rate coefficients, with the number of single events being related to the global symmetry of reactant and transition state of the elementary steps. This approach has been

applied to the catalytic cracking (Feng et al., 1992) and the hydrocracking (Baltanas et al., 1989; Svoboda et al., 1995; Martens and Froment, 1999; Schweitzer et al., 1999) of model components as well as catalytic cracking of a complex feedstock (Dewachtere et al., 1997, 1999). Indeed, provided the rate parameters of the elementary steps are independent of the chain length of the reacting hydrocarbon, the parameter values obtained on a set of well-chosen model components can be applied to complex mixtures of much heavier hydrocarbons (Thybaut et al., 2001). An obstacle in the use of such a model is often the enormous complexity of the reaction networks and the demand of a highly detailed analysis of the feed. However, a judicious relumping of the complex reaction network allows to circumvent the problem of an insufficiently detailed analysis, without losing sight of the underlying chemistry and, hence, also retaining the fundamental character of the kinetic parameters involved.

In this article a kinetic model for the hydrocracking of a hydrogenated vacuum gas oil will be derived by partially relumping the single event kinetic equations starting from the strategy described by Vynckier and Froment (1991) and, in particular, using so-called lumping coefficients (Dewachtere

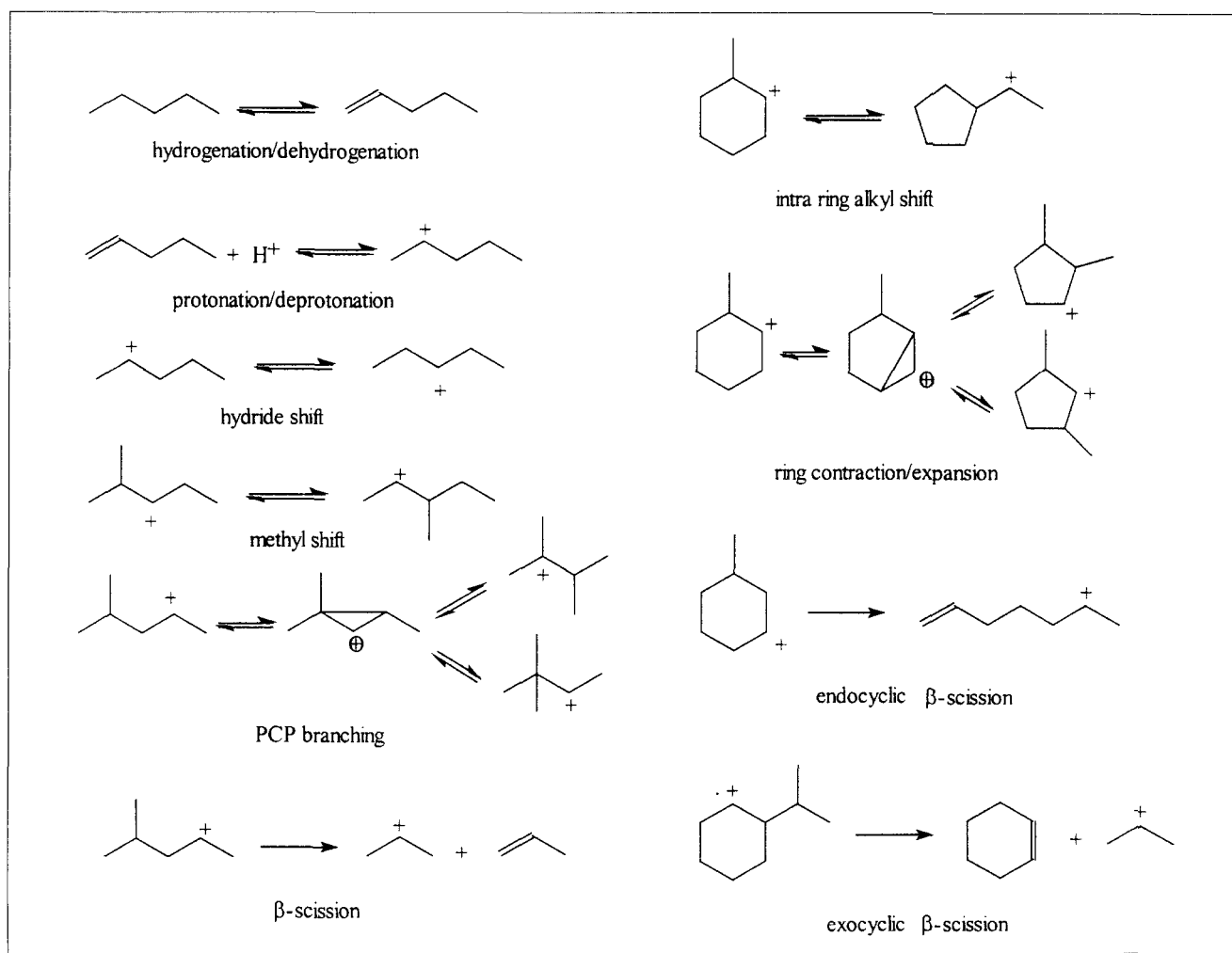


Figure 1. Metal and acid catalyzed steps of hydrocracking of alkanes and cycloalkanes.

et al., 1999). Froment and coworkers have indeed shown that the rate coefficient corresponding with a reaction in such a relumped network can be written as a combination of single event rate coefficient each of them multiplied with a different factor, the so-called lumping coefficient. For a particular lumping scheme, the values of these lumping coefficients depend only on the carbon number of the hydrocarbons of the reactant lump and can be calculated without the knowledge of the values for the single event rate coefficients starting from the network of elementary reaction steps.

Since the generation of this network requires excessive calculation times and memory capacities for heavy hydrocarbon feeds, a method is developed which enables to calculate the values for these lumping coefficients without generating the network of elementary steps. This method is based on the classification of the (cyclo)alkanes and carbenium ions involved in the network in structural classes. In order to illustrate the possible application of this approach an adiabatic three-phase reactor is simulated for the hydrocracking of a hydrogenated vacuum gas oil using kinetic parameters obtained from kinetic data obtained on Pt/US-Y for various alkane and cycloalkane key components.

Reaction Chemistry

Classical hydrocracking catalysts are bifunctional, that is, contain a hydrogenation function on an acidic carrier. The balance between hydrogenation and acid function determines strongly whether acid or metal catalyzed reactions predominate and, thus, determine the nature of the products formed (Langlois and Sullivan, 1971; Degnan and Kennedy, 1993). For a catalyst showing a strong hydrogenation activity, the reactions occurring on the acid sites will be rate determining. In the reaction scheme for this so-called ideal hydrocracking originally proposed by Weisz (1962) and Coonradt and Garwood (1964) alkanes or cycloalkanes dehydrogenate on the metal sites with formation of unsaturated (cyclo)alkenes, which in turn migrate to the Brønsted acid sites of the carrier

where they are protonated yielding carbenium ions. The metal catalyzed reactions and the elementary acid catalyzed reactions considered in the hydrocracking of alkanes and cycloalkanes are depicted in Figure 1. These comprise reactions such as protonation generating carbenium ions, hydride and alkyl shifts scrambling the position of the charge, or alkyl substituents, reactions such as PCP-branching and ring contraction altering the number of substituents and cracking reactions cleaving the C-C bond in β position of the positive charge. A weak acid function leads to a low content of feed isomers and mainly nonselective cracking on the metal sites, that is, hydrogenolysis. A weak hydrogenation activity on the other hand also reduces the isomerization selectivity due to the slow hydrogenation of (cyclo)alkene isomers leading to a high production of light products formed by acid catalyzed cracking of the (cyclo)alkyl carbenium ions formed out of these unsaturated hydrocarbons.

Physisorption of (cyclo)alkanes and (cyclo)alkenes into the zeolites pores (Steijns and Froment, 1981) precedes the reaction steps.

Single Event Kinetic Parameters

Implementation of the carbenium ion reaction rules for the hydrocracking of typical hydrocarbons present in an oil fraction results in huge reaction networks comprising thousands of intermediates and elementary steps. For example, hydrocracking of *n*-nonadecane yields 1981 alkanes, 25,065 alkenes, and 20,437 carbenium ions being subject to 25,065 hydrogenations, 25,065 dehydrogenations, 42,600 protonations, 42,600 deprotonations, 33,352 hydride shifts, 12,470 alkyl shifts, 15,970 PCP branchings, and 6,429 β -scissions. If with each of these reactions a different kinetic parameter is associated, determination of their values will become an impracticable task. A sensible reduction can, however, be attained for each of the reaction types when only the type of the carbenium ion, such as secondary or tertiary, is considered to have a relevant influence on the reaction rate. As a result, the

Table 1. Composite Preexponential Factors* and Complete Activation Energies**

Alkane Hydrocracking		Cycloalkane Hydrocracking	
Composite Activation Energy	kJ/mol	Composite Activation Energy	kJ/mol
$E_{PCP(s,s)}^{comp}$	43.7	$E_{Exo(s,s)}^{comp}$	77.6
$E_{PCP(s,t)}^{comp} = E_{PCP(t,s)}^{comp}$	36.5	$E_{Exo(s,t)}^{comp}$	59.1
$E_{PCP(t,t)}^{comp}$	31.8	$E_{Exo(t,s)}^{comp}$	57.5
$E_{Cr(s,s)}^{comp}$	69.5	$E_{Exo(t,t)}^{comp}$	24.3
$E_{Cr(s,t)}^{comp}$	57.0	$E_{RO(s,s)}^{comp}$	55.7
$E_{Cr(t,s)}^{comp}$	55.1	$E_{RO(s,t)}^{comp}$	37.4
$E_{Cr(t,t)}^{comp}$	29.5	$E_{LRO(t,s)}^{comp}$	38.5
		$E_{RO(t,t)}^{comp}$	30.6
Composite Preexponential Factor	kg _{cat} /(mol·s)	Composite Preexponential Factor	kg _{cat} /(mol·s)
$A_{PCP(s,s)}^{0,comp} = A_{PCP(s,t)}^{0,comp} = A_{PCP(t,s)}^{0,comp} = A_{PCP(t,t)}^{0,comp}$	1.82×10^9	$A_{Exo(s,s)}^{0,comp} = A_{Exo(s,t)}^{0,comp} = A_{Exo(t,s)}^{0,comp} = A_{Exo(t,t)}^{0,comp}$	2.59×10^{12}
$A_{Cr(s,s)}^{0,comp} = A_{Cr(s,t)}^{0,comp} = A_{Cr(t,s)}^{0,comp} = A_{Cr(t,t)}^{0,comp}$	2.59×10^{12}	$A_{RO(s,s)}^{0,comp} = A_{RO(s,t)}^{0,comp} = A_{RO(t,s)}^{0,comp} = A_{RO(t,t)}^{0,comp}$	2.06×10^{10}

* Calculated using transition state theory.

** Obtained from regression on gas phase hydrocracking data of alkane and cycloalkane model components for branching isomerization (PCP), β -scission (Cr), exocyclic cracking (Exo) and ring opening (RO).

possible effect of variations in skeletal structure of the carbenium ions on the rate by which they are consumed or produced is neglected with the exception of global symmetry. The influence of the latter on the reaction rate of the elementary steps can be taken into account by expressing an elementary step as a multiple of "single events," with the number of single events being defined as the ratio of the global symmetry numbers of reactant and activated complex. These so-called single event rate coefficients (Vynckier and Froment, 1991) only depend on the type of the reaction and product carbenium ion involved in the elementary step. Due to their low stability primary carbenium ions are excluded from the reaction network. Earlier work (Svoboda et al., 1995) showed that among the acid catalyzed reactions only the rearrangement and cracking of (cyclo)alkyl ions is kinetically significant while protonation/deprotonation and hydride shifts are quasi-equilibrated. Also, the total concentration of carbenium ions could be neglected compared to the total concentration of acid sites. As a result of these considerations only composite single event coefficients, that is, the product of the protonation equilibrium constant and the real single event rate coefficient appear in the rate equations. Their number amounts to 24: 3 for alkyl shifts, 3 for intraring alkyl shifts, 3 for PCP branching, 3 for ring contraction, 4 for acyclic β -scission, 4 for endocyclic β -scission and 4 for exocyclic β -scission. A reduction of the number of adjustable rate parameters is feasible via calculation of the composite pre-exponential factors from first principles (Martens et al., 2000a). The values for the remaining 24 composite activation energies had to be estimated from regressions on extensive experimental gas phase hydrocracking data on a Pt/US-Y zeolite for *n*-alkanes, that is, *n*-C₈, *n*-C₁₀, *n*-C₁₂, and cycloalkanes, that is, methylcyclohexane, ethylcyclohexane, and *n*-butylcyclohexane (Martens et al., 2000b). Values obtained for the composite pre-exponential factors and the composite activation energies for those reactions relevant within the frame of the relumped reaction network as defined in the next section are listed in Table 1. The resulting values were found to be statistically independent on the chain length of the investigated hydrocarbons and, hence, can be utilized to extrapolate the kinetics to heavier feedstocks (Martens et al., 2000a; Thybout et al., 2001).

Reaction Network, Kinetic Equations and Lumping Coefficients

Due to the restrictions imposed by the current analyzing techniques such as GC-MS on the determination of the identity of the molecules present in an oil fraction such as a vacuum gas oil, the individual hydrocarbons of the detailed reaction work generated by a computer implementation of the chemical reactions depicted in Figure 1 have to be assembled in eight lumps per carbon number: normal-, mono-, di- and tribranched alkanes and monoring-, diring-, triring-, and tetra-ring cycloalkanes reducing the fundamental reaction network of elementary steps to a relumped reaction scheme. Since the present work focuses on the modeling of the acid catalyzed reactions encountered in hydrocracking the metal catalyzed hydrogenation of the (poly)aromatic lumps into the corresponding cycloalkane lumps were not considered. The rate of conversion of the considered lumps into each other

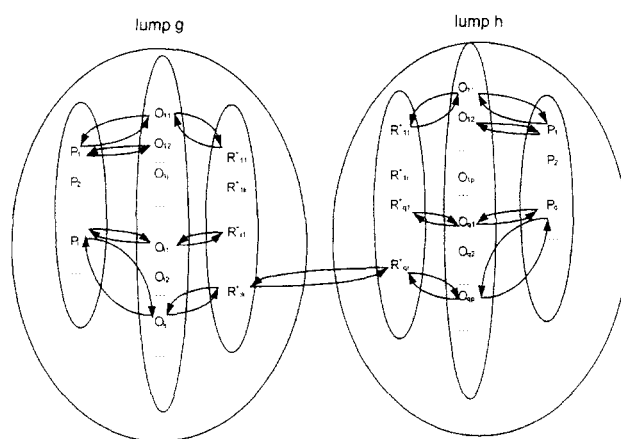


Figure 2. Relumping of (cyclo) alkanes and the corresponding (cyclo) alkenes and carbenium ions.

can be derived from the reaction network of elementary steps by summation of the rates of conversion of the individual molecules reassembled in the reactant lump into those of the product lump as is illustrated by Figure 2. Calculation of these rates involves the introduction of the following six hypotheses, the first three corresponding to ideal hydrocracking:

- Hydrogenation/dehydrogenation is in quasi equilibrium.
- Pseudo-steady state is assumed for the carbenium ions.
- Pseudo-steady state is assumed for the alkenes.
- The Langmuir physisorption coefficients for (cyclo) alkenes and (cyclo) alkanes are comparable.
- Protonation and deprotonation are in quasi equilibrium.
- The concentration of free acid sites approaches the total concentration of acid sites.

Since industrially hydrocracking occurs in liquid phase the relumped rate expressions as derived by Vynckier and Froment (1991) for gas-phase hydrocracking had to be modified by replacing the partial pressures with the fugacities of the lumps in the liquid phase resulting in the following expression, such as the isomerization rate of a lump *g* into a lump *h* in terms of the concentration of the lump, C_g , and of hydrogen C_{H_2}

$$r_{\text{isom}}(g;h) = \frac{k_{\text{isom}}^L(g;h) H_g^{\text{liq}} C_g}{p_i V_m \Phi_{L,H_2} \left(1 + \sum_f K_{L,f}^{\text{liq}} C_f \right) C_{H_2}} \quad (1)$$

with p_i the total pressure, V_m the molar volume of the liquid feed mixture, and Φ_{L,H_2} the fugacity coefficient for hydrogen in the liquid phase, which accounts for the nonideal behavior of this component in the liquid hydrocarbon mixture.

The lumped rate coefficient $k_{\text{isom}}^L(g;h)$ is a combination of products of the protonation equilibrium coefficients $\tilde{K}_{pr}(m_1)(m_1 = s \text{ or } t)$ and the single event rate coefficients $k_{\text{isom}}(m_1; m_2)$, that is, the composite single event coefficients, each of them multiplied with a so-called lumping coefficient

$$k_{\text{isom}}^L(g;h) = (LC)_{\text{isom}(s,s)}(g;h)\tilde{K}_{pr}(s)\tilde{k}_{\text{isom}}(s;s)C_t + (LC)_{\text{isom}(s,t)}(g;h) \times \tilde{K}_{pr}(s)\tilde{k}_{\text{isom}}(s;t)C_t + (LC)_{\text{isom}(t,s)}(g;h)\tilde{K}_{pr}(t)\tilde{k}_{\text{isom}}(t;s) \times C_t + (LC)_{\text{isom}(t,t)}(g;h)\tilde{K}_{pr}(t)\tilde{k}_{\text{isom}}(t;t)C_t \quad (2)$$

with C_t the total concentration of Brønsted acid sites of the zeolite used.

Values for the Henry coefficients for physisorption of the lump g in the liquid phase are obtained from the corresponding gas phase Henry coefficient via

$$H_g^{\text{liq}} = \frac{H_g^{\text{gas}}\Phi_{L,g}p_tV_m}{\Phi_{G,g}} \quad (3)$$

with $\Phi_{L,g}$ and $\Phi_{G,g}$ the fugacity coefficient of lump g in the liquid and gas phase. These fugacity coefficients are calculated using the Peng-Robinson equation of state (Peng and Robinson, 1976). For a given carbon number H_g^{gas} is considered to be independent on the skeletal structure of the hydrocarbons gathered in a lump resulting in a single Henry coefficient per lump. The value of the latter is obtained using the following correlations, relating the physisorption enthalpy and pre-exponential factor with carbon number, as obtained from literature physisorption data (Denayer and Baron, 1997; Denayer et al., 1998)

$$-\Delta H_{\text{phys},g}^0 = 6.51n + 8.21 \quad (\text{kJ/mol})$$

$$H_{0,g} = \exp(-0.757n - 17.4) \quad (\text{mol}/(\text{kg}_{\text{cast}} \text{Pa})) \quad (4)$$

with

$$H_g^{\text{gas}} = H_{0,g}e^{-\frac{\Delta H_{\text{phys},g}^0}{RT}} \quad (5)$$

The Langmuir coefficient for physisorption $K_{L,g}^{\text{liq}}$ of a lump g in the liquid phase is derived from the corresponding liquid-phase Henry coefficient divided by the saturation concentration $C_{\text{sat},g}$. Estimates for the latter are obtained from the pore volume of the zeolite and the molar volume of the lump.

Values for the lumping coefficients in Eq. 2 associated with each of the reactions of the lumped network can be calculated from the generated reaction network of elementary steps as a sum comprising a number of terms corresponding with each of the elementary isomerization steps converting a carbenium ion of type m_1 generated out of the hydrocarbons of lump g into carbenium ions of type m_2 corresponding with hydrocarbons of lump h (Vynckier and Froment, 1991)

$$(LC)_{\text{isom}(m_1,m_2)}(g;h) = \sum_{i \in g} \sum_{k \in g} \sum_{q \in h} \sum_{r \in h} \frac{n_{e,ikqr}\sigma_{O_{ij}}}{\sigma R_{ik}^+} \tilde{K}_{\text{isom}}(O_{ij}, O_r) K_{DH,ij} y_{i,g} \quad (6)$$

As illustrated by Figure 2, the sum is taken over all reactant carbenium ions with index k originating from all cyclo (alkanes) with index i belonging to lump g , and over all possible product ions with index r resulting in (cyclo)alkanes with index q belonging to lump h . Each of these terms comprises the mol fraction of a hydrocarbon in lump g , $y_{i,g}$, the equilibrium coefficient, $K_{DH,ij}$ for dehydrogenation of a (cyclo)alkane P_i into one of the corresponding alkenes O_{ij} , the equilibrium coefficient $\tilde{K}_{\text{isom}}(O_{ij}, O_r)$ for isomerization alkene O_{ij} and a chosen reference alkene O_r (Baltanas et al., 1989; Froment, 1991), the global symmetry numbers; $\sigma_{O_{ij}}$ and $\sigma_{R_{ik}^+}$ of the alkene O_{ij} and the reactant carbenium ion R_{ik}^+ and the number of single events $n_{e,ikqr}$ for the isomerization reaction considered. Note, that the resulting values do not require the knowledge of the single event rate coefficients, but merely depend on the choice of the lumps and the network of elementary steps and, hence, can be calculated independently of the rate parameters. Since calculation of the lumping coefficients does, however, require the knowledge of $y_{i,g}$ and, hence, of the composition of a lump, all hydrocarbons within a lump are considered at equilibrium with $y_{i,g}$ the equilibrium mol fraction. The lumping coefficients obtained from Eq. 6 and the generated network show an Arrhenius type temperature dependency and are a function of the number of carbon atoms of the molecules within the reactant lump, as shown by Figure 3 for $LC_{PCP(s,t)}$ of a dibranched alkane lump into a monobranched alkane lump. The temper-

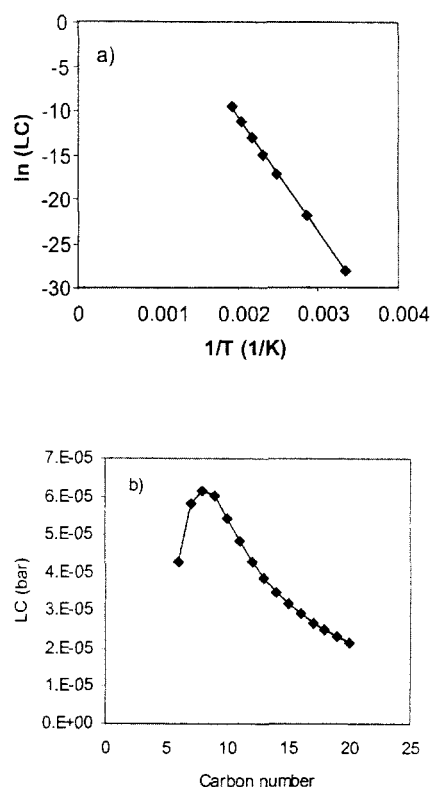


Figure 3. (a) Evolution of $(LC)_{PCP(s,t)}(diP_{20}, moP_{20})$ with temperature and (b) evolution of $(LC)_{PCP(s,t)}(diP_n, moP_n)$ at $T=500$ K with carbon number n .

ature effect mainly originates from the van't Hoff temperature dependence of the value of the hydrogenation/dehydrogenation equilibrium coefficient since both the values for $K_{\text{isom}}(O_{ij}, O_r)$ and $y_{i,g}$ alter only slightly with changing temperature.

Lumping Coefficients Without the Generation of a Network: Structural Class Based Calculation

Although feasible in theory, a calculation of the lumping coefficients for hydrocracking of heavy feedstocks from Eq. 6 is hampered by the excessive amount of CPU-time and memory required for the generation of the reaction network. To circumvent this problem a calculation method is developed that does not require this time consuming network generation and is based on a simple rearrangement of Eq. 6, that is:

$$(LC)_{\text{isom}(m_1, m_2)}(g; h) = \frac{N_{\text{isom}(m_1, m_2)} K_{\text{ref}, g}^*(n; T)}{K_g^*(n; T)} \quad (7)$$

with

$$K_{\text{ref}, g}^*(n; T) = e^{-\frac{\Delta \tilde{G}_f^0(O_r) + \Delta \tilde{G}_f^0(H_2)}{RT}} \quad (8)$$

$$K_g^*(n; T) = \sum_{i \in g} \frac{e^{-\frac{\Delta \tilde{G}_f^0(P_i)}{RT}}}{\sigma_{P_i}} \quad (9)$$

$$N_{\text{isom}/Cr(m_1, m_2)} = \sum_{i \in g} \sum_{k \in g} \sum_{q \in h} \sum_{r \in h} \frac{n_{c,ikqr}}{\sigma_{R_{ik}} \sigma_{H_2}} \quad (10)$$

The factor $K_{\text{ref}, g}^*(n; T)$ can be related with the equilibrium coefficient for formation of the reference alkene and hydrogen from the pure elements, while $K_g^*(n; T)$ is the sum of the equilibrium coefficients for the formation of all (cyclo)alkanes P_i of lump g . The temperature independent factor $N_{\text{isom}(m_1, m_2)}$ is related to the total number of single events of the lumped reaction. The calculation of each of these factors is based on the use of Benson's group contribution method (Benson et al., 1969; Reid et al., 1988) as a source of thermodynamic data for the (cyclo)alkanes and (cyclo)alkenes of the network due to the lack of reliable literature data for long-chain hydrocarbons. In this method each hydrocarbon is considered as a combination of distinctive structural groups whereby the values for the thermodynamic properties can be found additively from those of the corresponding structural groups. The method does not account for the influences of the enthalpy of formation of next-nearest neighbors with the exception of gauche interactions.

The calculation of $K_{\text{ref}, g}^*$ for each lump using Eq. 8 is straightforward using thermodynamic data obtained from Benson's method for the reference alkene O_r while for hydrogen literature data (Reid et al., 1988) is used. For each carbon number five $K_{\text{ref}, g}^*$ factors corresponding with the alkane, mono-, di-, tri- and tetracycloalkane lumps have to be calculated.

Calculation of the factor K_g^* defined by Eq. 9 based on Benson's group contribution method to obtain values for

$\Delta \tilde{G}_f^0(P_i)$, the single event standard Gibbs enthalpy of formation, that is, symmetry contribution not included, allows to derive a mathematical expression for K_g^* as a function of temperature and carbon number for each lump. According to Benson's rules, the values for the enthalpy and the specific heat capacity of a (cyclo)alkane depend only on the type, (that is, primary, secondary, tertiary, and quaternary) of each carbon atom of the molecule; the number and the type of ring structures; and on the number of gauche interactions between the carbon-carbon bonds of the molecule. As a consequence, all hydrocarbons within a lump can easily be subdivided into several hydrocarbon classes with equal $\Delta \tilde{G}_f^0(P_i)$ and global symmetry number σ_{P_i} . This strategy reduces the large number of (cyclo)alkanes within a lump into a limited number of structural classes whereby each class consists of a number of different hydrocarbons which, nevertheless, all have the same values for the global symmetry, enthalpy, single event entropy and specific heat capacity when using Benson's method. If, furthermore, for each of those classes, the number of hydrocarbons belonging to such a class, $\#_i$, can be derived as a function of the carbon number, the factor K_g^* can be calculated via

$$K_g^*(n; T) = \sum_i^{n \text{ classes}} \frac{\#_i}{\sigma_i} e^{-\frac{n_{p,i} \Delta \tilde{G}_{f,p}^0}{RT}} e^{-\frac{n_{s,i} \Delta \tilde{G}_{f,s}^0}{RT}} e^{-\frac{n_{t,i} \Delta \tilde{G}_{f,t}^0}{RT}} e^{-\frac{n_{q,i} \Delta \tilde{G}_{f,q}^0}{RT}} e^{-\frac{n_{c5,i} \Delta \tilde{G}_{f,c5}^0}{RT}} e^{-\frac{n_{c6,i} \Delta \tilde{G}_{f,c6}^0}{RT}} e^{-\frac{n_{gch,i} \Delta H_{f,gch}^0}{RT}} \quad (11)$$

with $n_{p,i}$, $n_{s,i}$, $n_{t,i}$, $n_{q,i}$, the number of primary, secondary, tertiary and quaternary carbon atoms, $n_{c5,i}$, $n_{c6,i}$ the number of five and six membered rings, σ_i the global symmetry number, and $n_{gch,i}$ the minimum number of gauche interactions for the alkane structural class i of lump g . In addition $\Delta \tilde{G}_{f,p}^0$, $\Delta \tilde{G}_{f,s}^0$, $\Delta \tilde{G}_{f,t}^0$ and $\Delta \tilde{G}_{f,q}^0$ represent Benson's group contributions to the single event standard Gibbs enthalpy at temperature T for a primary, secondary, tertiary, and quaternary carbon atom, $\Delta \tilde{G}_{f,c5}^0$ and $\Delta \tilde{G}_{f,c6}^0$ those for 5 and 6-rings and $\Delta H_{f,gch}^0$ the contribution to the enthalpy value associated with one alkane gauche interaction. By way of example, the six structural classes for the monobranched alkane lumps are listed in Table 2. In a similar way, all di- and tribranched alkanes and all mono-, di-, tri- and tetraring cycloalkanes can be categorized in a limited number of structural classes. The classification of all alkanes considered only hydrocarbons with

Table 2. Structural Classes of Single Branched Alkanes

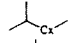
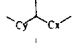
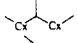
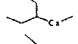
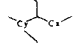
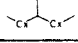
Alkane Class	$n_{p,i}$	$n_{s,i}$	$n_{t,i}$	$n_{q,i}$	σ_i	$n_{gch,i}$	No. of Alkanes $\#_i$
	3	$n-4$	1	0	27	1	1
	3	$n-4$	1	0	27/2	2	($n-6$)/2 n even ($n-5$)/2 n odd
	3	$n-4$	1	0	27	2	1 n even
	3	$n-4$	1	0	27	3	0 n odd
	3	$n-4$	1	0	27/2	3	($n-8$)/2 n even ($n-9$)/2 n odd
	3	$n-4$	1	0	27	3	0 n even 1 n odd

Table 3. Structural Classes of Carbenium Ions Contributing to $N_{PCP(s,t)}(diP_n;moP_n)$

Carbenium Ion Class R_{ik}^+	Global Symmetry No. $\sigma_{R_{ik}^+}$	No. of Ions, $\#_i$	$n_{e,ikqr}$	$\frac{n_{e,ikqr}\#_i}{\sigma_{R_{ik}^+}\sigma_{H_2}}$
	243	1	18	$\frac{9}{243}$
	81	$n-6$	12	$\frac{6(n-6)}{81}$
	81/2	1	6	$\frac{6}{81}$
	81	1	6	$\frac{3}{81}$
	81/2	$n-9$	6	$\frac{6(n-9)}{81}$

a maximum of three substituents, while no substituents larger than ethyl groups were considered. For cycloalkanes, only one substituent larger than a methyl group was allowed with a maximum of four substituents. For di-, tri- and tetra-ring cycloalkanes, only molecules with six-membered rings were considered and percondensed structures were not selected. The strategy followed to calculate the factor $N_{isom/Cr(m_1,m_2)}$ defined by Eq. 10 for all the isomerization and cracking steps within the lumped reaction network is illustrated for the (s,t) PCP isomerization of a dibranched alkane lump, diP_n , to a monobranched alkane lump moP_n . In order to obtain the value of $N_{PCP(s,t)}(diP_n;moP_n)$, the global symmetry number of all possible secondary dibranched reactant ions with n carbon atoms being able to react according to a PCP step with formation of a tertiary monobranched ion have to be determined together with the number of single events for each of these steps. The result of this classification for the PCP example reaction is shown in Table 3 containing all possible reactant carbenium ions divided into several structural

classes. The structure of the carbenium ions within each group is listed in the first column of this table, while the following columns contain the global symmetry number, the number of ions within each group and the number of single events for the isomerization of these ions.

Applying Eq. 10 on the data listed in this table, an expression for $N_{PCP(s,t)}(diP_n;moP_n)$ can be obtained as a function of the carbon number by calculating

$$\frac{n_{e,ikqr}\#_i}{\sigma_{R_{ik}^+}\sigma_{H_2}} \quad \text{with} \quad \sigma_{H_2} = 2 \quad (12)$$

for each structural carbenium ion class. The expressions resulting from Eq. 12 for each of the structural reactant carbenium ion classes are listed in the last column of Table 3. Addition of all these expressions results in an expression for

Table 4. Structural Classes of Carbenium Ions Contributing to $N_{Cr(s,s)}(moN_n;moN_p;diP_{n-p})$

Carbenium Ion Class	Global Symmetry No. $\sigma_{R_{ik}^+}$	No. of Ions	$n_{e,ikqr}$	$\frac{n_{e,ikqr}\#_i}{\sigma_{R_{ik}^+}\sigma_{H_2}}$
	81/4	$n-p-6$	1	$\frac{2(n-p-6)}{81}$
	81/8	$(n-p-6)(n-p-7)/2$	1	$\frac{8(n-p-6)(n-p-7)}{81}$
	243/2	1	1	$\frac{1}{243}$
	81/2	$(n-p-6)$	1	$\frac{(n-p-6)}{81}$
	81/4	$(n-p-6)$	1	$\frac{2(n-p-6)}{81}$
	81/8	$(n-p-6)(n-p-7)/2$	1	$\frac{8(n-p-6)(n-p-7)}{81}$
	243/2	1	1	$\frac{1}{243}$
	81/2	$n-p-6$	1	$\frac{(n-p-6)}{81}$

$$N_{PCP(s,t)}(diP_n; moP_n)$$

$$N_{PCP(s,t)}(diP_n; moP_n) = \frac{12(n-7)+6}{81} \quad n \geq 10 \quad (13)$$

which is only valid for $n \geq 10$ since from ten carbon atoms on all possible carbenium ion classes contributing to $N_{PCP(s,t)}(diP_n; moP_n)$ are represented.

In a similar way expressions for the factor defined by Eq. 10 can be derived for each isomerization and cracking reaction of the alkane, as well as the cycloalkane lumps of the chosen relumped reaction network. By way of example $N_{Cr(m_1, m_2)}(g; h, l)$ corresponding with the cracking of a monocycloalkane lump moN_n yielding a lighter monocycloalkane lump moN_p and a dibranched alkane lump diP_{n-p} . The classes of all reactant carbenium ions reacting according to this reaction are listed in Table 4. The expressions resulting from applying Eq. 12 to each of the carbenium ion classes shown in this table can be found in the last column of this table. Combining these expressions leads to the following expression for $N_{Cr(s,s)}(moN_n; moN_p; diP_{n-p})$

$$N_{Cr(s,s)}(moN_n; moN_p; diP_{n-p}) = \frac{4 + 12(n-p-6) + 24(n-p-6)^2}{243} \quad 8 \leq p \leq n-8 \quad (14)$$

The definition of the global symmetry number and the calculation of its value has been explained in detail by Baltanas et al. (1989). The determination of the expressions for the number of carbenium ions for each structural class will be illustrated for the second ion class of Table 4. Carbenium ions belonging to this class can react according to



with $x = p-7$ since the cycloalkane formed contains p carbon atoms. The olefin is split off and has $n-p$ carbon atoms with a skeletal structure consisting of a main chain of $n-p-2$ carbon atoms with $n-p-4$ carbon atoms on which each of the two methyl groups can be placed. Since the first class in Table 4 already contains those carbenium ions with one methyl group positioned at the end of the main chain and the reactant carbenium ion should be a secondary cation, only $(n-p-6)$ possible positions remain to place the first methyl group and $(n-p-7)$ for the second. Since switching both methyl groups leads to the same olefin, the number of possible olefins formed and, hence, the number of possible reactant carbenium ions amounts to $(n-p-6)(n-p-7)/2$. In an analogous way, expressions for the number of ions belonging to the other classes tabulated have been derived. Once expressions for $K_{ref,g}^*(n;T)$ and $K_g^*(n;T)$ are available for all lumps and expressions for $N_{isom(m_1, m_2)}(g;h)$ or $N_{cr(m_1, m_2)}(g;h,l)$ are derived for each reaction of the lumped network, overall expressions for the lumping coefficients can be obtained by appropriately combining the expressions derived for these factors using Eq. 7. The lumping coefficient for (s,t) PCP isomerization for the

(s,t) isomerization of lump diP_n to moP_n is given by

$$(LC)_{PCP(s,t)}(diP_n; moP_n) = \frac{12(n-7)+6}{81} \frac{K_{ref,Par}^*}{K_{di}^*} \times n \geq 10 \quad (15)$$

Similarly, the lumping coefficient for (s,s) β -scission of a monocycloalkane lump moN_n yielding a monocycloalkane lump moN_p and a dibranched alkane lump diP_{n-p} is given by

$$(LC)_{Cr(s,s)}(moN_n; moN_p; diP_{n-p}) = \frac{4 + 12(n-p-6) + 24(n-p-6)^2}{243} \frac{K_{ref,moNap}^*}{K_{MoN}^*} \quad 8 \leq p \leq n-8 \quad (16)$$

Since, for example, Eq. 15 is only valid for carbon numbers larger than 10, while Eq. 16 is only valid in the range $8 \leq p \leq n-8$, additional formulae have to be developed for the example reaction considered when dealing with smaller hydrocarbons. These calculations, however, do not differ fundamentally from the approach used to obtain the general expressions and require only an appropriate selection of the structural (cyclo)alkane or carbenium ion classes contributing to K_{di}^* and $N_{PCP(s,t)}(diP_n; moP_n)$ for a certain carbon number.

As can be expected, the values calculated with, for example, Eq. 15 and the related expressions derived for $n < 10$, are identical to those calculated using the network of elementary steps, exhibiting the same temperature and chain-length dependence as that shown in Figure 3, since the structural class-based calculation method is based on the same hypotheses as those incorporated in the network-based calculations, that is, it does not introduce new assumptions or simplifications.

Moreover, looking at the mathematical expressions for the lumping coefficients, some features like the decrease of $(LC)_{PCP(s,t)}(diP_n; moP_n)$ with carbon number for $n > 9$ can be understood more easily. The evolution of $N_{PCP(s,t)}(diP_n; moP_n)$ with carbon number, depicted in Figure 4, clearly shows a linear increase, see Eq. 13 for a dibranched alkane lump diP_n with a carbon number above 9. For carbon numbers lower than 10, however, a nonlinear increase of $N_{PCP(s,t)}(diP_n; moP_n)$ is noticed. Since $K_{ref,Par}^*/K_{di}^*$ decreases continuously in a nonlinear way, see Figure 4, a maximum is observed in the value of the lumping coefficient $(LC)_{PCP(s,t)}(diP_n; moP_n)$, viz. Figure 3b. The monotonous decrease of $(LC)_{PCP(s,t)}(diP_n; moP_n)$ for $n > 9$ is also intuitively clear from the definition of the lumping coefficient in Eq. 6 and, more specifically, from the different influence of the carbon number on the value of the equilibrium mol fraction $y_{i,g}$ and on the total number of elementary steps contributing to the lumping coefficient. The equilibrium mol fraction $y_{i,g}$ is expected to decrease almost proportionally with the number of alkanes in a lump, which is proportional to the second power of the carbon number for the diP_n -lump. The number of reactions contributes to $(LC)_{PCP(s,t)}(diP_n; moP_n)$ viz. Table

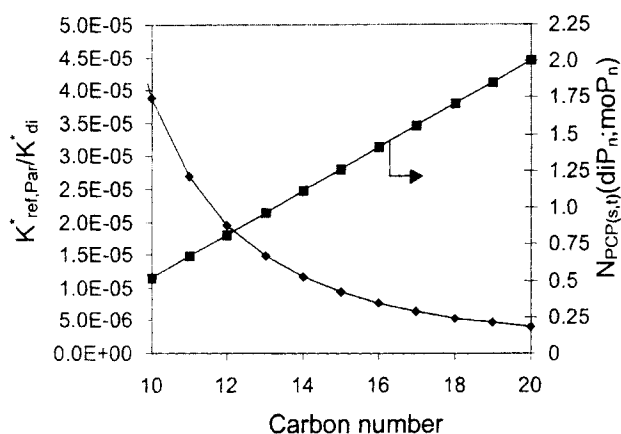


Figure 4. Ratio of $K_{ref,Par}^*$ to K_{di}^* (♦) and $N_{pCP(s,t)}(diP_n;moP_n)$ (■) as a function of carbon number n as calculated with Eqs. 8, 11 and 13.

3, and on the other hand, increases linearly with carbon number. Hence, a certain carbon number on the number of carbenium ions contributes to $(LC)_{pCP(s,t)}(diP_n;moP_n)$ and increases linearly with carbon number n , while the equilibrium mol fraction of the corresponding cycloalkanes in the lump decreases in a quadratic way with n and a decrease of the lumping coefficient is expected.

Similar to the example discussed above, expressions, applicable at any lumped chain length of the hydrocarbons, are derived to obtain values for the lumping coefficients for all possible reactions within the lumping scheme considered.

Application: Hydrocracking of a Hydrogenated Vacuum Gas Oil in an Adiabatic Three-Phase Reactor

In the second half of this article the results are discussed of the simulation of the hydrocracking of a hydrogenated vacuum gas oil in an industrial reactor performed to demonstrate the straightforward incorporation of the derived kinetic equations into a classical model for a three-phase adiabatic reactor and the ability is illustrated of fundamental models to supply detailed information and insight concerning the effect of, for example, the process conditions on product composition and quality without requiring an excessive number of rate parameters of computational efforts.

Feedstock, products, reactor geometry and process conditions

The feedstock used in the simulation consists of a hydrogenated vacuum gas oil whose composition is derived from that of a partially hydrogenated vacuum gas oil (VGO) by incorporating the content of aromatic fractions into those of the corresponding cycloalkane fractions and is briefly characterized by the following composition: 14 wt. % n -alkanes, 11 wt. % single branched alkanes, 1 wt. % dibranched alkanes, 33 wt. % monocycloalkanes, 25 wt. % dicycloalkanes, 10% tricycloalkanes and 6 wt. % tetracycloalkanes. The carbon number of the hydrocarbons ranges from 14 to 33, while the boiling point range of the original partially hydrogenated

VGO is 580–750⁺ K. The product hydrocarbons are grouped in terms of the traditional hydrocracker products LPG, naphtha, and middle distillates. The typical carbon number ranges and boiling point ranges, identifying each of these product fractions, are listed in Table 5. The lumped reaction network for hydrocracking of this feedstock results in 144 alkane and 89 cycloalkane lumps that are subject to 172 isomerizations, 3,242 acyclic β -scissions, 4,446 cyclic β -scissions, and 172 ring opening reactions. The treat gas used in the reactor simulations consists of 90 % mol. hydrogen, 9 % mol. methane and 1% of nitrogen while the reactor geometry, catalyst properties, and inlet conditions are listed in Table 6. Thermodynamic equilibrium was assumed between the gas and liquid phase at the reactor inlet.

Reactor model

Industrially, the hydrocracking of petroleum fractions is performed in a multiphase adiabatic fixed-bed reactor comprising three phases: a fixed bed of catalyst pellets, a vapor phase, and a liquid phase flow concurrently downward. The liquid phase comprises feed hydrocarbons with dissolved gases such as hydrogen and light hydrocarbons, while the gas phase mainly consists of hydrogen and evaporated feed components. The flow regimes in such a reactor can be classified into a low interaction regime (trickle flow regime) and a high interaction regime (pulse, spray, and bubble flow regimes). Trickle flow is observed at low gas and liquid flow rates, with the liquid phase flowing down the packing in the form of droplets, films, and rivulets, while the continuous gas phase occupies the remaining porous space. Although laboratory-scale reactors are generally operating in the trickle-flow regime for industrial three-phase downflow operations, the pulsing flow regime is also reported as a commonly observed flow regime. This regime is established at moderate liquid flow rates and moderate to high gas-flow rates.

A point of attention in the operation of trickle bed reactors is the degree of utilization of the catalyst. In contrast with laboratory-scale reactors for sufficiently high liquid velocities, a complete wetting of the catalyst can be expected for industrial-scale trickle-bed reactors operating in the trickle flow regime (Al-Dahhan and Dudukovic, 1995), while the internal contacting is usually equal to unity due to capillary effects (Al-Dahhan et al., 1997). For the conditions used in the simulations, the reactor is found to operate in the transition regime between trickle flow and pulse flow. The wetting efficiency calculated from correlations developed for high pressure/temperature laboratory scale trickle-bed reactors (Ruecker and Agkerman, 1987; Ring and Missen, 1991; Al-Dahhan and Dudukovic, 1995) is found to be close to unity at the conditions in the simulation.

The model used to describe the hydrodynamics is a one-dimensional heterogeneous model with both gas and liquid phase in plug flow (Froment et al., 1994) leading to a continuity equation of a component i of the gas phase from the form

$$\frac{1}{\Omega} \frac{dF_{iG}}{dz} = -K_L a'_v \left(\frac{C_{iG}}{H_i} - C_{iL} \right) \quad i = 1, \dots, N$$

at $z = 0 \quad F_{iG} = F_{iG}^0$ (17)

Although such an ideal flow distribution is not achieved in most laboratory-scale reactors operating under trickle flow conditions, Shah (1979) consider deviations from plug flow to be negligible in most industrial trickle-bed reactors.

Since complete wetting of the catalyst is assumed, the molar flow rate of a component i in the gas phase can only change due to mass transfer to or from the liquid phase. Using the two film model to describe the mass transfer allows the molar flux for a component i to be written as

$$N_i = K_L \left(\frac{C_{iG}}{H_i} - C_{iL} \right) \quad (18)$$

with

$$\frac{1}{K_L} = \frac{1}{k_G H_i} + \frac{1}{k_L} \quad (19)$$

the overall resistance to mass transfer which is composed of the resistances to mass transfer in the two films. The Henry coefficients H_i are calculated from the distribution coefficients K_i 's obtained from a gas-liquid equilibrium calculation,

$$H_i = K_i \frac{\rho_G}{\rho_L} \frac{M_{w,L}}{M_{w,G}} \quad (20)$$

The volumetric liquid-side mass-transfer coefficient $k_L a'_v$ is derived from a correlation proposed by Sato et al. (1972). The volumetric gas-side mass-transfer coefficient $k_G a'_v$ is derived from Reiss' (1967) correlation.

The liquid phase is considered to be in the plug-flow regime and is in contact with both the vapor and solid phase. For the conditions used, the resistance to mass and heat transfer between the catalyst surface and the liquid bulk is found to be negligible while possible temperature gradients inside the catalyst particle are not considered. As a consequence, two terms appear in the righthand side of the continuity equation for a component i in the liquid phase reflecting the net production rate and mass transfer

$$\frac{1}{\Omega} \frac{dF_{iL}}{dz} = \rho_B \sum_{j=1}^{N_r} \eta_j S_{ji} r_j (C_{iL}, \dots, T_s) + K_L a'_v \left(\frac{C_{iG}}{H_i} - C_{iL} \right) \quad (21)$$

at $z=0 \quad F_{iL} = F_{iL}^0 \quad i=1, \dots, N$

with η_j the effectiveness factor of reaction j calculated as the ratio of the rate of reaction with pore diffusion resistance obtained from integration of the intrinsic reaction rate along the radial concentration profile within the catalyst particle and the reaction rate in absence of diffusion, that is, at liquid bulk concentrations. The stoichiometry coefficient matrix S gives the factors S_{ji} .

The concentration gradients inside the catalyst particle are taken into consideration by the following continuity equa-

tions for a component i , in case of a spherical particle

$$\frac{D_{ic}}{\xi^2} \frac{d}{d\xi} \left(\xi^2 \frac{dC_{is}}{d\xi} \right) = \rho_s \sum_j S_{ji} r_j (C_{is}, \dots, T_s) \quad (22)$$

with boundary conditions

$$\begin{aligned} \text{at } \xi=0 \quad \frac{dC_{is}}{d\xi} &= 0 \\ \text{at } \xi = \frac{d_p}{2} \quad C_{is} &= C_{iL} \end{aligned} \quad (23)$$

The diffusivity of each component in the liquid phase is calculated using the method of Wilke-Chang. The effective diffusivity D_{ic} accounts for the porosity ϵ_s and for the tortuosity of the catalyst particle τ .

The reaction is operated adiabatically. An energy equation is considered for each of the three phases with the catalyst particles assumed as being isothermal. The energy transfer between gas and liquid phase consists of a conductive heat flux and a contribution due to the enthalpy transport induced by the interphase mass transfer. The energy equation for the vapor phase is given by

$$\begin{aligned} u_{sG} \rho_G C_{p,G} \frac{dT_G}{dz} &= h_G a'_v (T_I - T_G) + \sum_{i=1}^N N_i a'_v C_{p,Gi} (T_G - T_I) \\ \text{at } z=0 \quad T_G &= T_G^0 \end{aligned} \quad (24)$$

The heat consumed or released by vaporization or condensation of a component i due to its transfer from the liquid phase to the gas phase or vice versa is incorporated in the energy equation for the liquid phase

$$\begin{aligned} u_{sL} \rho_L C_{p,L} \frac{dT_L}{dz} &= \rho_B \sum_{j=1}^{N_r} \eta_j r_j (C_{iL}, \dots, T_L) (-\Delta H_{r,j}) \\ &+ h_L a'_v (T_I - T_L) + \sum_{i=1}^N N_i a'_v (\Delta H_{iv} + C_{p,Li} (T_I - T_L)) \\ \text{at } z=0 \quad T_L &= T_L^0 \end{aligned} \quad (25)$$

with η_j the effectiveness factor for reaction j . The reaction rates, r_j in Eqs. 21, 22 and 25 are the rates of the various reactions within the lumped reaction network derived. As explained in the first part of this article, values for these rates are obtained using a Langmuir-Hinshelwood type of rate expression cfr. Eq. 1 relating the reaction rate with the measurable concentrations of the hydrocarbon lumps. The rate coefficients in these expressions are found by applying Eq. 2 and using values for the rate parameters of the various types of kinetic relevant elementary reaction steps determined from regressions on experimental hydrocracking data obtained on a Pt/US-Y catalyst for several paraffinic and naphthenic model components (Martens et al., 2000a, b) while values for the lumping coefficients in turn are calculated using expressions similar to Eqs. 13 and 14.

The two-phase pressure drop is expressed in terms of the single phase pressure drop for the liquid δ_L and the gas phase δ_G using Larkins' equation (Larkins et al., 1961)

$$-\frac{dp_t}{dz} = (\delta_L + \delta_G) 10 \left[\frac{0.416}{\left(\log_{10} \sqrt{\frac{\delta_L}{\delta_G}} \right)^2 + 0.666} \right]$$

at $z = 0 \quad p_t = p_t^0$ (26)

with the single phase flow pressure drops δ_L and δ_G calculated from the Ergun equation.

Estimation of physical properties

The critical temperature, critical pressure, critical volume, standard enthalpy of formation, Gibbs enthalpy of formation, and the ideal gas specific heat capacity of the lumps are calculated from the values for the individual hydrocarbons using well-established mixing rules (Reid et al., 1988). Values for the physical and thermodynamic properties of the individual alkanes and cycloalkanes are taken from literature when available or estimated using group contribution methods like Joback's, Fedors' and Benson's method. The acentric factor is calculated by means of the Lee-Kesler method (Lee and Kesler, 1975). Other properties like the enthalpy of reaction in the liquid phase, the enthalpy of vaporization, the specific heat capacity and density of the liquid and gas phase, and the fugacity coefficients in liquid and gas phase required for the calculation of the Henry coefficients are calculated based on the Peng-Robinson equation of state. Binary interaction parameters for hydrogen used in the Peng-Robinson equation of state to account for the solubility of hydrogen in a liquid hydrocarbon mixture were obtained from the correlation proposed by Moysan et al. (1983). The viscosity of both gas and liquid phase is derived from the method of Brulé and Star-

ling (1984) while the binary diffusion coefficient in the liquid phase is obtained from the Wilke-Chang method (Wilke and Chang, 1955).

Integration method

The integration of the 204 continuity equations for the gas phase, the 204 continuity equations of the liquid phase, the energy equations for both phases, and the pressure drop equation in the axial direction is performed using Gear's method (Lapidus and Seinfeld, 1971). Although one continuity equation can be eliminated using the mass balance, all continuity equations are integrated simultaneously, the mass conservation criterion is being used as control only. The intraparticle integration is carried out with an orthogonal spline collocation method (Villadsen and Michelsen, 1978). The initial guess of the concentration profiles in the catalyst particle is further updated using a Newton-Raphson method until the required accuracy is obtained. All simulations were performed on an IBM RISC-6000 397 and required between 5 and 25 min of CPU time. The main computational effort corresponds to the calculation of the effectiveness factors since reactor calculations performed with all η_i 's fixed at unity require a CPU time of a few minutes or even less than a minute.

Assessment of gas-liquid and internal transport limitations

For the reactor geometry and inlet conditions of Table 6, a reactor calculation results in a conversion of the C_{18}^+ hydrocarbon fraction of 99 wt. %. The heat produced by the overall exothermic hydrocracking reactions hereby induces a difference in temperature between the gas and liquid phase of about 2.5 K at 0.5 m, while beyond 2 m, a constant difference of 1 K is established. The overall temperature increase between inlet and outlet for the liquid phase amount to 5.5 K. It should be noted, however, that, due to the saturated nature of the feedstock, the considerable heat produced by the hydrogenation of aromatics present in a typical hydrocracker

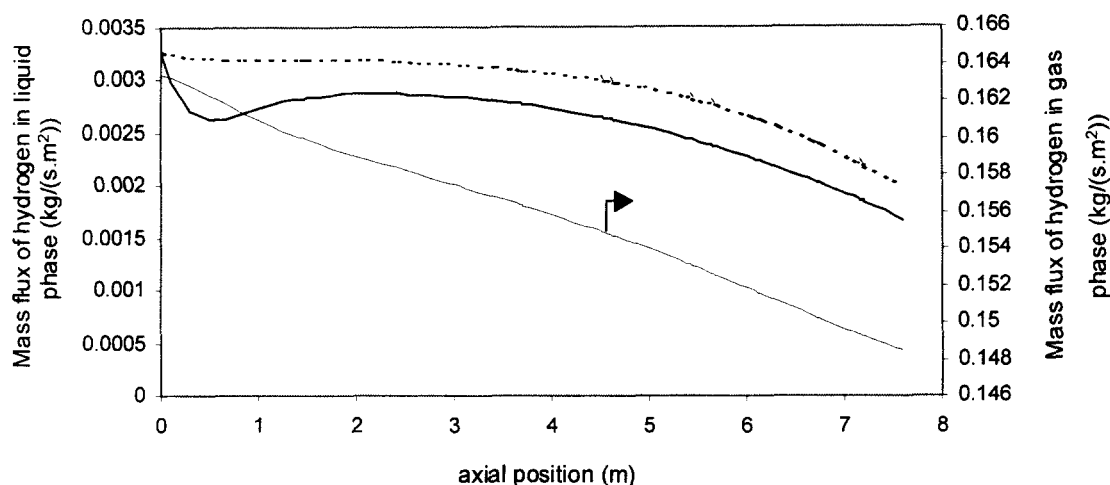


Figure 5. Hydrogen mass flux in both phases (full lines) and hydrogen mass flux in the liquid phase if saturated with hydrogen (dashed line) as a function of axial position.

Hydrocracking of a hydrogenated VGO at the conditions of Table 6 using reactor model Eqs. 17–26, kinetic Eqs. 1–6 and kinetic parameters listed in Table 1 obtained on a Pt/US-Y zeolite.

feed is excluded here. Accounting for the content of aromatics in the original partial hydrogenated VGO, an adiabatic temperature rise associated with the total hydrogenation of this aromatic fraction amounts to almost 100 K.

The evolution of the mass flux of hydrogen in the liquid and gas phase are shown in Figure 5 together with the mass flux of hydrogen in the liquid phase in equilibrium with the gas phase. As a consequence of the interfacial mass-transfer resistance, the liquid phase is not completely saturated with hydrogen. A slight minimum is noticed in the liquid-phase hydrogen mass flux near the inlet due to the fast cracking of the heavy alkanes and cycloalkanes in the first section of the reactor. At a higher axial position, the mass fluxes of hydrogen in both phases decrease monotonously. In contrast with hydrogen, no resistance is noticed towards mass transfer from gas to liquid phase or vice versa for the various hydrocarbon lumps indicating that the rate for mass transfer is considerably higher than that of the acid catalyzed reactions. As far as hydrocracking of saturated feedstocks not involving hydrogenation of aromatics is concerned, equilibrium is established between all hydrocarbons in the gas and liquid phase while only a minor resistance to gas-liquid mass transfer is noticed for hydrogen.

In addition the absence of strong intraparticle diffusion limitations is illustrated via the values for the effectiveness factors of some isomerization and ring opening reactions are listed in Table 7 at different axial positions. Only for those reactions transforming the heavier and more reactive alkane or cycloalkane lumps, some resistance to mass transfer inside the catalyst particle is noticed considering the values below 0.8 for the effectiveness factor, such as the branching isomerization of *n*-heptacosane into its monobranched isomers. It should be mentioned, however, that at an axial position of 2 m, at which $\eta = 0.91$ is already 65% of *n*-C₂₇ and has been consumed, while, at $z = 3$ m and $\eta = 0.77$, the conversion already amounts to 95%. The initial values higher than unity for the effectiveness factors of the four example reactions are caused by the initial positive net rates of formation of the reactant lumps of these reactions leading, as a consequence of the limited intraparticle diffusion limitations, to small con-

Table 6. Reactor Geometry, Catalyst Properties and Inlet Conditions Used in the Simulations

Reactor Geometry	
Reactor diameter, m	2.82
Reactor length, m	7.625
Catalyst Properties	
Catalyst particle diameter, m	1.3×10^{-3}
Porosity of catalyst, m^3/m^3_p	0.65
Bulk density of bed, kg_{cat}/m^3	800
Catalyst density, kg_{cat}/m^3_p	400
Catalyst mass, kg_{cat}	19,000
Tortuosity	3.7
Conditions	
Inlet temperature, K	540
Inlet pressure, MPa	12
LHSV, $m^3/(m^3_{cat} \cdot h)$	3.8
Liquid flow rate, m^3/d	2,175
Gas flow rate Nm^3/d	1,100,000

centration gradients in the catalyst particle and to concentration inside the particle surpassing those of the liquid bulk. Once molecules within these lumps start to disappear instead of being formed, the effectiveness factor of the four reactions decreases and eventually drops below unity.

Composition profiles in the bed

Figure 6 shows the evolution along the axial coordinate of the mass fluxes of hydrocarbon fractions representing the classical refinery products, as defined in Table 5. The LPG (C₃-C₄), naphtha (C₅-C₉) and middle distillate (C₁₀-C₁₈) mass flux increase monotonously along the reactor, with the latter being the most abundant product. Some small differences are noticed in the product quality of both naphtha and middle distillate (see Figure 7), while the former product stream contains larger amounts of alkanes compared to the latter, the share of isoalkanes in the middle distillates is markedly higher than that of the C₅-C₉ fraction. The high content of isoalkanes in all fractions is a well known feature of hydrocracking with large pore zeolites such as a US-Y, on which the kinetic parameters used in the present simulations are obtained. Differences are also noticed in the evolution of the composition of both product fractions along the reactor: whereas the composition of the naphtha fraction hardly changes, cracking of the long-chain feed alkanes induces an increase of the isoalkane fraction in the middle distillates together with a strong decrease of the monocycloalkane fraction and an increase of the dicycloalkanes in the first meter of the reactor.

Table 5. Definition of Product Fractions in Terms of Carbon Number Range and Corresponding Boiling Point Range

Product	Carbon No.	Boiling Point K	(°F)
LPG	C ₃ -C ₄	< 315	(< 100)
Naphtha	C ₅ -C ₉	315-425	(100-300)
Middle distillates	C ₁₀ -C ₁₈	425-620	(300-660)
Residue	C ₁₈ ⁺	> 620	(> 660)

Table 7. Effectiveness Factor of Branching Isomerization and Ring Opening Reactions

Axial Position (m)	Effectiveness Factor, η			
	$nP_{27} \rightarrow moP_{27}$	$diP_{22} \rightarrow moP_{22}$	$moN_{30} \rightarrow moP_{30}$	$triN_{20} \rightarrow diN_{20}$
1	1.03	1.10	1.05	1.09
2	0.91	1.06	0.98	1.04
3	0.77	1.03	0.94	1.03
4	0.62	1.01	0.90	1.01

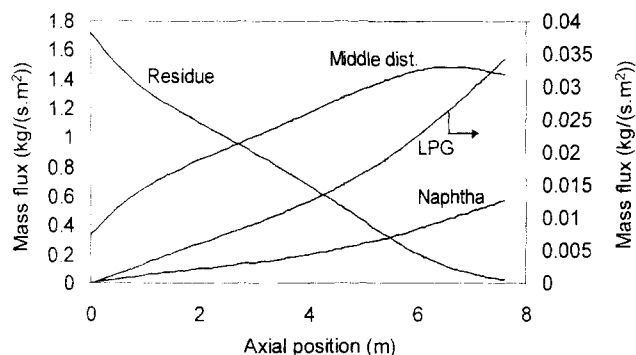


Figure 6. Mass fluxes of the different product fractions as a function of axial position.

Hydrocracking of a hydrogenated VGO at the conditions of Table 6 using model Eqs. 17–26, kinetic Eqs. 1–6 and kinetic parameters listed in Table 1 obtained on a Pt/US-Y zeolite.

Obviously, the model is capable of providing information in far more detail, as shown in Figures 6 and 7. By way of example, the evolution of the liquid concentration of various monoring cycloalkane lumps along the axial coordinate is shown in Figure 8. This illustrates some typical features such as the high content of C_6 and C_7 monoring cycloalkanes in the cracked products. This is a consequence of the well known predominance of the fast (t,t) exocyclic cracking mode (Sullivan et al., 1961; Egan et al., 1962), also better known as a “paring” reaction. Similar profiles for each of the 203 hydro-

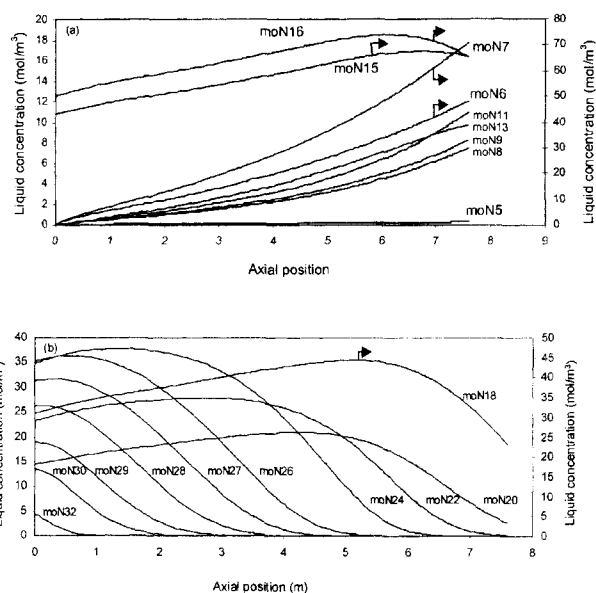


Figure 8. Liquid bulk concentration of (a) C_5 – C_{16} monocyclic cycloalkane lumps and (b) C_{18} – C_{32} monocyclic cycloalkane lumps as a function of axial position.

Simulation of hydrocracking of a hydrogenated VGO at the conditions of Table 6 using model Eqs. 17–26, kinetic Eqs. 1–6 and kinetic parameters listed in Table 1 obtained on a Pt/US-Y zeolite.

carbon lumps deliver a highly detailed picture of the evolution of the various fractions along the reactor, thus permitting monitoring of the influence of variations in temperature, pressure, and hydrogen partial pressure and to arrive at optimal operating conditions for a given feedstock, catalyst, and reactor geometry.

Conclusions

A kinetic model incorporating the detailed reaction chemistry has been implemented into an adiabatic multiphase fixed-bed reactor model for hydrocracking of a hydrogenated VGO. Starting from the knowledge of the kinetics of the elementary steps, a relumping of the individual molecules to a degree corresponding with the state-of-the-art analytical techniques and with the actual product specifications was performed. The rate coefficients for a reaction within this relumped network can be expressed as a combination of single event rate coefficients, associated with the elementary reaction steps, and so-called lumping coefficients of which the value depends on the choice of the lumps and the reaction temperature, but not on the single event coefficients.

To avoid the excessive calculation times needed for the generation of the network of elementary reaction steps, a method is developed to allow values for each lumping coefficient to be obtained without the generation of this network.

In this method, every component (either reactant, product or intermediate carbenium ion) is assigned to a so-called structural class. Each structural class is characterized by thermodynamic properties such as enthalpy, single event entropy,

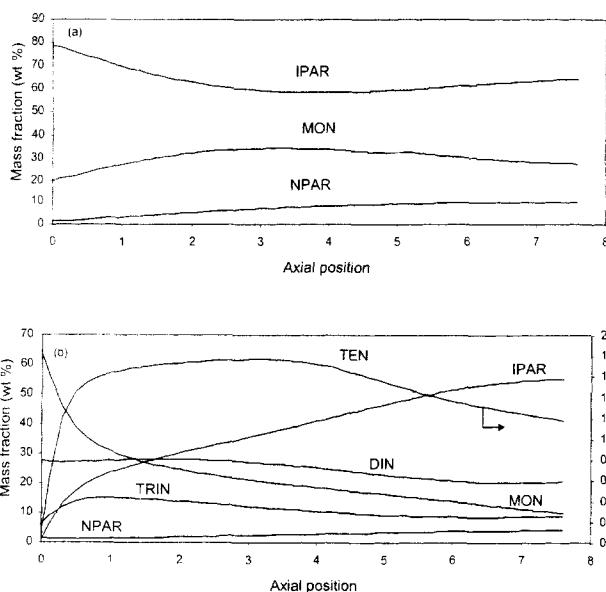


Figure 7. Composition of (a) the C_5 – C_9 fraction and (b) the C_{10} – C_{18} fraction as a function of axial position.

Hydrocracking of a hydrogenated VGO at the conditions of Table 6 using model Eqs. 17–26, kinetic Eqs. 1–6 and kinetic parameters listed in Table 1 obtained on a Pt/US-Y zeolite. (NPAR: n-alkanes; IPAR: isoalkanes; MON: monocycloalkanes; DIN: dicycloalkanes; TRIN: tricycloalkanes; TEN: tetracycloalkanes).

specific heat capacity and global symmetry. When applying Benson's group contribution method to calculate the latter, each structural class is characterized by the number of primary, secondary, tertiary, and quaternary carbon atoms, the number of five and six membered rings, the global symmetry number and the minimum number of gauche interactions. This structural class based method is equivalent with the calculation method using the generated reaction network, as long as Benson's method is used to obtain the necessary thermodynamic data in both approaches.

Determination of a relatively limited number of kinetic parameters from experiments with well-chosen model components allows to simulate with the model the hydrocracking of heavy hydrocarbon mixtures as complex as a vacuum gas oil. These simulations reveal that the gas-liquid transfer, as well as diffusion inside the catalyst's pores, occurs at a rate potentially much higher than that of the acid catalyzed reactions at the conditions considered. The level of detail provided by the model concerning the composition and quality of the various products is far beyond that of the classical lumped models, without, however, requiring excessive computational efforts. Hence, the fundamental kinetic model used in this work may provide a powerful tool in the design, optimization and control of an industrial hydroprocessing unit.

Acknowledgment

This research has been done as a part of the program "Interuniversitaire Attractiepolen (funded by the Belgian Government), Dienst van de Eerste Minister - Federale Diensten voor Wetenschappelijke, Technische en Culturele Aangelegenheden."

Notation

a'_v = gas-liquid interfacial area per unit reactor volume, m^2/m^3
 a''_v = liquid-solid interfacial area per unit reactor volume, m^2/m^3
 $A_{\text{isom}/\text{cr}}^{\text{comp}}(m_1, m_2)$ = composite preexponential factor for isomerization or cracking of a carbenium ion of type m_1 into an ion of type m_2 , $\text{kg}_{\text{cat}}/(\text{mol} \cdot \text{s})$
 C_{iG} = molar concentration of i in the gas bulk, mol/m^3
 C_{iL} = molar concentration of i in the liquid bulk, mol/m^3
 C_{is} = molar concentration of i inside the solid, mol/m^3
 C_{is}^s = molar concentration of fluid reactant i at the external surface of solid, mol/m^3
 C_g, C_f = concentration of lump g or f in the liquid bulk, mol/m^3
 C_{H_2} = concentration of hydrogen in the liquid phase, mol/m^3
 $C_{p,G}$ = specific heat capacity of gas phase, $\text{J}/(\text{kg} \cdot \text{K})$
 $C_{p,L}$ = specific heat capacity of liquid phase, $\text{J}/(\text{kg} \cdot \text{K})$
 C_t = total concentration of Brønsted acid sites, $\text{mol}/\text{kg}_{\text{cat}}$
 d_p = equivalent particle diameter, m
 d_r = reactor diameter, m
 D_{ic} = effective diffusivity of component i for transport in a pseudocontinuum, $m^2/(\text{m}_{\text{cat}} \cdot \text{s})$
 $E_{\text{isom}/\text{cr}}^{\text{comp}}(m_1, m_2)$ = composite activation energy for isomerization or cracking of a carbenium ion of type m_1 into n ion of type m_2 , J/mol
 F = molar flow rate, mol/s
 h_L, h_G = liquid and gas phase heat-transfer coefficients, $\text{J}/(\text{m}^2 \cdot \text{s} \cdot \text{K})$
 h_f = heat-transfer coefficient for the film surround-

ing a catalyst particle, $\text{J}/(\text{m}^2 \cdot \text{s} \cdot \text{K})$
 H_i = Henry's law coefficient, $m^3/\text{Pa} \cdot \text{mol}$
 H_g^{gas} = Henry coefficient for adsorption of lump g in gas phase, $\text{mol}/(\text{kg}_{\text{cat}} \cdot \text{Pa})$
 H_g^{liq} = Henry coefficient for adsorption of a lump g in liquid phase, $m^3/\text{kg}_{\text{cat}}$
 k_G = mass-transfer coefficient from gas to gas-liquid interface, based on concentration driving force, $m^3_G/(\text{m}^2 \cdot \text{s})$
 $k_{\text{isom}}^L(g; h)$ = lumped rate coefficient for isomerization of lump g into lump h , Pa/s
 $k_{\text{isom}}(m_{ik}; m_{qr})$ = single event rate constant for isomerization of a carbenium ion of type m_{ik} to a carbenium ion of type m_{qr} , s^{-1}
 k_l = liquid-solid mass-transfer coefficient, $m^3_l/(\text{m}^2 \cdot \text{s})$
 k_L = mass-transfer coefficient from gas-liquid interface to liquid bulk, based on concentration driving force, $m^3_L/(\text{m}^2 \cdot \text{s})$
 K_L = overall mass-transfer coefficient in terms of liquid concentration gradient, $m^3_l/(\text{m}^2 \cdot \text{s})$
 $K_{L,f}^{\text{liq}}$ = Langmuir coefficient for adsorption of a lump f in the liquid phase, m^3_f/mol
 $K_{DH,ij}$ = equilibrium constant for dehydrogenation of alkane P_i with formation of alkene O_{ij} , Pa
 $\tilde{K}_{\text{isom}}(O_r, O_{ij})$ = single event equilibrium constant for isomerization of O_r into O_{ij} , that is, symmetry contributions for the entropy not included
 $\tilde{K}_{p_r}(m_{ik})$ = single event equilibrium coefficient for protonation/deprotonation of the reference alkene with formation of a carbenium ion of type m_{ik} , $\text{kg}_{\text{cat}}/\text{mol}$
 $(LC)_{\text{isom}}(m_1; m_2)(g; h)$ = lumping coefficient for isomerization of carbenium ions of type m_1 of lump g into carbenium ions of type m_2 of lump h , Pa
 M_w = molecular mass, kg/mol
 n = carbon number
 $ne_{ik,qr}$ = number of single events
 N_i = rate of transfer of i from the gas bulk to the liquid bulk, $\text{mol}/(\text{m}^2 \cdot \text{s})$
 p_i = total pressure, Pa
 P_i = alkane or cycloalkane with index i
 $r_{\text{isom}}(g; h)$ = rate of the isomerization of lump g to lump h , $\text{mol}/(\text{kg}_{\text{cat}} \cdot \text{s})$
 r_j = reaction rate of reaction j , $\text{mol}/(\text{kg}_{\text{cat}} \cdot \text{s})$
 S_{ij} = stoichiometric coefficient for component i in reaction j
 T = absolute temperature, K
 V_m = molar volume of feed mixture, m^3/mol
 $y_{i,g}$ = (equilibrium) mol fraction of hydrocarbon P_i in lump g
 z = axial coordinate in the reactor, m

Greek letters

δ_G = frictional pressure drop per unit length for gas flow only, Pa/m
 δ_L = frictional pressure drop per unit length for liquid flow only, Pa/m
 ΔH_v = heat of vaporization of species i , J/mol
 $\Delta H_r, \square \Delta H_{r,j}$ = standard reaction enthalpy (or reaction j), J/mol
 $\Delta \tilde{G}_f^0$ = single event standard Gibbs enthalpy of formation, J/mol
 ϵ = bed void fraction, m^3_f/m^3
 η_j = effectiveness factor of reaction j
 ξ = radial pellet coordinate, m
 μ = viscosity, $\text{Pa} \cdot \text{s}$
 ρ_B = catalyst bulk density, $\text{kg}_{\text{cat}}/m^3$
 ρ_G = gas density, kg/m^3
 ρ_L = liquid density, kg/m^3
 ρ_c = density of the catalyst, $\text{kg}_{\text{cat}}/m^3_p$
 σ = global symmetry number
 Ω = cross section of reactor, m^2

$\Phi_{l,g}$ = fugacity coefficient for lump g in the gas phase
 $\Phi_{G,g}$ = fugacity coefficient for lump g in the liquid phase

Literature Cited

- Al-Dahhan, M. H., and M. P. Dudukovic, "Catalyst Wetting Efficiency in Trickle Bed Reactors at High Pressure," *Chem. Eng. Sci.*, **50**, 2377 (1995).
- Al-Dahhan, M. H., F. Larachi, M. P. Dudukovic, and A. Laurent, "High-Pressure Trickle-Bed Reactors: A Review," *Ind. Eng. Chem. Res.*, **36**, 3292 (1997).
- Baltanas, M. A., K. K. Van Raemdonck, G. F. Froment, and S. R. Mohedas, "Fundamental Kinetic Modeling of Hydroisomerization and Hydrocracking on Noble-Metal-Loaded Faujasites: 1. Rate Parameters for Hydroisomerization," *Ind. Eng. Chem. Res.*, **28**, 899 (1989).
- Benson, S. W., F. R. Cruikshank, D. M. Golden, G. R. Haugen, H. E. O'Neal, A. S. Rodgers, R. Shaw, and R. Walsh, "Additivity Rules for Estimation of Thermodynamical Properties," *Chem. Rev.*, **69**, 279 (1969).
- Broadbeldt, L. J., S. M. Stark, and M. T. Klein, "Computer Generated Pyrolysis Modeling: On-the-Fly Generation of Species, Reactions and Rates," *Ind. Eng. Chem. Res.*, **33**, 790 (1994).
- Brulé, M. R., and K. E. Starling, "Thermophysical Properties of Complex Systems: Applications of Multiproperty Analysis," *Ind. Eng. Chem. Process Des.*, **23**, 833 (1984).
- Cicarelli, P., G. Astarita, and A. Gallifuoco, "Continuous Kinetic Lumping of Catalytic Cracking Processes," *AIChE J.*, **38**, 1038 (1992).
- Clymans, P. J., and G. F. Froment, "Computer-Generation of Reaction Paths and Rate Equations in the Thermal Cracking of Normal and Branched Paraffins," *Comp. & Chem. Eng.*, **8**, 137 (1984).
- Coonradt, H. L., and W. E. Garwood, "Mechanism of Hydrocracking," *Ind. Eng. Chem. Proc. Des.*, **3**, 38 (1964).
- Degnan, T. F., and C. R. Kennedy, "Impact of Catalyst Acid/Metal Balance in the Hydroisomerization of Normal Paraffins," *AIChE J.*, **39**, 607 (1993).
- Denayer, J. F. M., and G. V. Baron, "Adsorption of Normal and Branched Paraffins in Faujasite Zeolites NaY, HY, Pt/NaY and USY," *Adsorption*, **3**, 1 (1997).
- Denayer, J. F., G. V. Baron, J. A. Martens, and P. A. Jacobs, "Chromatographic Study of Adsorption of n -Alkanes on Zeolites at High Temperatures," *J. Phys. Chem. B*, **102**, 3077 (1998).
- Dewachtere, N. V., G. F. Froment, I. Vasalos, N. Markatos, and N. Skandalis, "Advanced Modeling of Riser-Type Catalytic Cracking Reactors," *Appl. Thermal. Eng.*, **17**, 837 (1997).
- Dewachtere, N. V., F. Santaella, and G. F. Froment, "Application of a Single-Event Kinetic Model in the Simulation of an Industrial Riser Reactor for the Catalytic Cracking of Vacuum Gas Oil," *Chem. Eng. Sci.*, **54**, 3653 (1999).
- Egan, C. J., G. E. Langlois, and R. J. White, "Selective Hydrocracking of C9 to C12-Alkylcyclohexanes on Acidic Catalysts: Evidence for the Paring Reaction," *J. Am. Chem. Soc.*, **84**, 1204 (1962).
- Feng, W., E. Vynckier, and G. F. Froment, "Single Event Kinetics of Catalytic Cracking," *Ind. Eng. Chem. Res.*, **32**, 2997 (1992).
- Froment, G. F., "Kinetic Modeling of Complex Catalytic Reactions," *Rev. de l'Institut Français du Pét.*, **46**, 491 (1991).
- Froment, G. F., G. A. Depauw, and V. Vanrysselberghe, "Kinetic Modeling and Reactor Simulation in Hydrodesulfurization of Oil Fractions," *Ind. Eng. Chem. Res.*, **33**, 2975 (1994).
- Jacob, S. M., B. Gross, S. E. Voltz, and V. W. Weekman, "A Lumping and Reaction Scheme for Catalytic Cracking," *AIChE J.*, **22**, 701 (1976).
- Hillewaert, L. P., J. L. Dierickx, and G. F. Froment, "Computer Generation of Reaction Schemes and Rate Equations for Thermal Cracking," *AIChE J.*, **34**, 17 (1988).
- Krambeck, F. J., "Thermodynamics and Kinetics of Complex Mixtures," *Chem. Eng. Sci.*, **49**, 4179 (1994).
- Langlois, G. E., and R. F. Sullivan, "Chemistry of Hydrocracking," *Adv. Chem. Ser.*, **97**, 3666 (1971).
- Lapidus, L., and J. H. Seinfeld, *Numerical Solution of Ordinary Differential Equations*, Academic Press, New York and London (1971).
- Larkins, R. P., R. R. White, and D. W. Jeffrey, "Two-Phase Concurrent Flow in Packed Beds," *AIChE J.*, **47**, 231 (1961).
- Laxminarasimhan, C. S., R. P. Verma, and P. A. Ramachandran, "Continuous Lumping Model for Simulation of Hydrocracking," *AIChE J.*, **42**, 2645 (1996).
- Lee, B. I. and M. G. Kesler, "A Generalized Thermodynamic Correlation Based on Three-Parameter Corresponding States," *AIChE J.*, **21**, 510 (1975).
- Liguras, D. K., and D. T. Allen, "Structural Models for Catalytic Cracking: 1. Model Compounds Reactions," *Ind. Eng. Chem. Res.*, **28**, 665 (1989a).
- Liguras, D. K. and D. T. Allen, "Structural Models for Catalytic Cracking: 2. Reactions of Simulated Oil Mixtures," *Ind. Eng. Chem. Res.*, **28**, 674 (1989b).
- Marin, G. B., and G. F. Froment, "The Development and Use of Rate Equations for Catalytic Refinery Processes," *Stud. Surf. Sci. Cat.*, **53**, 497 (1990).
- Martens, G. G., and G. F. Froment, "Kinetic Modeling of Paraffins Hydrocracking Based Upon Elementary Steps and the Single Event Concept," *Stud. Surf. Sci. Cat.*, **122**, 333 (1999).
- Martens, G. G., G. B. Marin, P. A. Jacobs, J. A. Martens, and G. V. Baron, "A Fundamental Kinetic Model for Hydrocracking of C₈-C₁₂ Alkanes on Pt/US-Y Zeolites," *J. Catal.*, **195**, 253 (2000a).
- Martens, G. G., J. W. Thybaut, and G. B. Marin, "Single Event Parameters for Hydrocracking of Cycloalkanes on Pt/US-Y Zeolites," *Ind. Eng. Chem. Res.*, **40**, 1832 (2000b).
- Moysan, J. M., M. J. Huron, H. Paradowski, and J. Vidal, "Prediction of the Solubility of Hydrogen in Hydrocarbon Solvents Through Cubic Equations of State," *Chem. Eng. Sci.*, **38**, 1085 (1983).
- Peng, D. Y., and D. B. Robinson, "A New Two-Constant Equation of State," *Ind. Eng. Chem. Fundam.*, **15**, 59 (1976).
- Quader, S. A., S. Singh, W. H. Wiser, and G. R. Hill, "Hydrocracking of Petroleum Oil," *J. Inst. Petrol.*, **56**, 187 (1970).
- Quann, R. J., and S. B. Jaffe, "Structure-Oriented Lumping: Describing the Chemistry of Complex Hydrocarbon Mixtures," *Ind. Eng. Chem. Res.*, **31**, 2483 (1992).
- Quann, R. J., and S. B. Jaffe, "Building Useful Models of Complex Reaction Systems in Petroleum Refining," *Chem. Eng. Sci.*, **51**, 1615 (1996).
- Reid, C. R., J. M. Prausnitz, and B. E. Poling, *The Properties of Gases and Liquids*, McGraw-Hill, New York (1988).
- Reiss, L. P., "Concurrent Gas-Liquid Contacting in Packed Bed Columns," *Ind. Eng. Chem. Process Des. Dev.*, **6**, 486 (1967).
- Ring, Z. E., and R. W. Missen, "Trickle-Bed Reactors: Tracer Study of Liquid Hold-Up and Wetting Efficiency at High Temperature and Pressure," *Can. J. Chem. Eng.*, **69**, 1016 (1991).
- Ruecker, C. M., and A. Agkerman, "Determination of Wetting Efficiency for a Trickle-Bed Reactor at High Temperatures and Pressures," *Ind. Eng. Chem. Res.*, **26**, 164 (1987).
- Sato, Y., H. Hirose, F. Takahashi, and M. Toda, "Performance of Fixed-Bed Catalytic Reactor with Cocurrent Gas-Liquid Downflow," *First Pacific Chemical Engineering Congress*, p. 187 (1972).
- Schweitzer, J. M., P. Galtier, and D. Schweich, "A Single Kinetic Model for the Hydrocracking of Paraffins in a Three-Phase Reactor," *Chem. Eng. Sci.*, **54**, 2441 (1999).
- Shah, Y. T., *Gas-Liquid-Solid-Reactor Design*, McGraw-Hill, New York (1979).
- Stangeland, B. E., and J. R. Kitrell, "Jet Fuel Selectivity in Hydrocracking," *Ind. Eng. Chem. Process. Des. Dev.*, **11**, 16 (1972).
- Steijns, M., and G. F. Froment, "Hydroisomerization and Hydrocracking: 3. Kinetic Analysis of Rate Data for n -Decane and n -Dodecane," *Ind. Chem. Product Res. Dev.*, **20**, 660 (1981).
- Sullivan, R. F., C. J. Egan, G. E. Langlois, and R. P. Sieg, "A New Reaction that Occurs in the Hydrocracking of Certain Aromatic Hydrocarbons," *J. Amer. Chem. Soc.*, **83**, 1156 (1961).
- Svoboda, G. D., E. Vynckier, B. De Brabandere, and G. F. Froment, "Application of a Single-Event Kinetic Model to Octane Hydrocracking on a Pt/US-Y Zeolite," *Ind. Eng. Chem. Res.*, **34**, 3793 (1995).
- Thybaut, J. W., G. B. Marin, G. V. Baron, P. A. Jacobs, and J. A. Martens, "Alkene Protonation Enthalpy Determination from Fundamental Kinetic Modeling of Alkane Hydroconversion on Pt/H-(US) Y-Zeolite," *J. Catal.*, in press (2001).

- Villadsen, J., and M. C. Michelsen, "Solution of Differential Equation Models by Polynomial Approximation," Prentice Hall, Englewood Cliffs, NJ (1978).
- Vynckier, E., and G. F. Froment, "Modeling of the Kinetics of Complex Processes Based upon Elementary Steps," *Kinetic and Thermodynamic Lumping of Multicomponent Mixtures*, G. Asarita and S. I. Sandler, eds., Elsevier Science Publishers, Amsterdam, p. 131 (1991).
- Watson, B. A., M. T. Klein, and R. H. Harding, "Mechanistic Modeling of n-Heptane Cracking on HZSM-5," *Ind. Eng. Chem. Res.*, **35**, 1506 (1996).
- Watson, B. A., M. T. Klein, and R. H. Harding, "Catalytic Cracking of Alkylbenzenes: Modeling the Reaction Pathways and Mechanisms," *Appl. Catal. A*, **160**, 13 (1997a).
- Watson, B. A., M. T. Klein, and R. H. Harding, "Mechanistic Modelling of a 1-Phenyloctane/n-Hexadecane Mixture on Rare Earth Y Zeolite," *Ind. Eng. Chem. Res.*, **36**, 2954 (1997b).
- Weekman, V. W., and D. M. Nace, "Kinetics of Catalytic Cracking Selectivity in Fixed, Moving, and Fluid Bed Reactors," *AIChE J.*, **16**, 397 (1970).
- Weisz, P. B., "Polyfunctional Heterogeneous Catalysis," *Adv. Cat.*, **13**, 137 (1962).
- Wilke, C. R., and P. Chang, "Correlations of Diffusion Coefficients in Dilute Solution," *AIChE J.*, **1**, 264 (1955).

Manuscript received Apr. 2, 2000, and revision received Nov. 1, 2000.